

Syracuse University

SURFACE

Physics

College of Arts and Sciences

2-2-2008

Nematic and Polar Order in Active Filament Solutions

A. Ahmadi
Syracuse University

Tanniemola B. Liverpool
University of Leeds

M. Cristina Marchetti
Syracuse University

Follow this and additional works at: <https://surface.syr.edu/phy>



Part of the [Physics Commons](#)

Recommended Citation

arXiv:cond-mat/0507590v1

This Article is brought to you for free and open access by the College of Arts and Sciences at SURFACE. It has been accepted for inclusion in Physics by an authorized administrator of SURFACE. For more information, please contact surface@syr.edu.

Nematic and Polar order in Active Filament Solutions

A. Ahmadi¹, T. B. Liverpool², and M. C. Marchetti¹

¹*Physics Department, Syracuse University, Syracuse, NY 13244, USA and*

²*Department of Applied Mathematics, University of Leeds, Woodhouse Lane, Leeds LS2 9JT, UK*

(Dated: February 2, 2008)

Using a microscopic model of interacting polar biofilaments and motor proteins, we characterize the phase diagram of both homogeneous and inhomogeneous states in terms of experimental parameters. The *polarity* of motor clusters is key in determining the organization of the filaments in homogeneous isotropic, polarized and nematic states, while motor-induced bundling yields spatially inhomogeneous structures.

Soft active systems are exciting examples of a new type of condensed matter where stored energy is continuously transformed into mechanical work at microscopic length scales. A realization of this are polar filaments interacting with associated molecular motors in the cell cytoskeleton^{1,2}. These systems are characterized by a variety of dynamic and stationary states which the cell accesses as part of its cycle^{3,4,5}.

There have been a number of recent theoretical studies of the collective dynamics of isotropic and polarized solutions of active filaments. These include numerical simulations^{4,5}, mesoscopic mean-field kinetic equations^{7,9,10,11}, and hydrodynamic equations where the system is described in terms of a few coarse-grained fields whose dynamics is inferred from symmetry considerations^{12,13,14,15}. Previous work has focused on how motor activity renders homogeneous states unstable to the formation of spatial structures, such as bundles, vortices or asters. In this article we study the profound effect of motor activity on the possible homogeneous states of the system¹⁶. We also find important differences in the nature of the instabilities from these homogeneous phases. Starting from a microscopic model of interacting rigid filaments, we characterize a phase diagram of homogeneous and inhomogeneous states of active filaments in terms of experimentally variable parameters. We find in particular that the formation of a non-equilibrium polarized phase at low densities can be driven by motor *polarity* without the need for filament polymerization^{12,15}.

We describe the system by a concentration of polar filaments $f(\mathbf{r}, \hat{\mathbf{n}}, t)$ in two dimensions ($d = 2$), modeled as hard rods of *fixed* length ℓ and diameter b ($\ell \gg b$) at position \mathbf{r} with filament polarity characterized by a unit vector $\hat{\mathbf{n}}$, and a density of motor clusters $m(\mathbf{r}, t)$ at position \mathbf{r} . The filament and motor concentrations satisfy the equations

$$\partial_t f = -\nabla \cdot \mathbf{J}_f - \mathcal{R} \cdot \mathcal{J}, \quad (1)$$

$$\partial_t m = -\nabla \cdot \mathbf{J}_m \quad (2)$$

where $\mathcal{R} = \hat{\mathbf{n}} \times \partial_{\hat{\mathbf{n}}}$ and the translational ($\mathbf{J}_f, \mathbf{J}_m$) and rotational (\mathcal{J}) currents have diffusive, excluded volume and active contributions. The rotational current is $\mathcal{J} = \mathcal{J}^D + \mathcal{J}^X + \mathcal{J}^A$, with a diffusive current $\mathcal{J}^D(\mathbf{r}, \hat{\mathbf{n}}, t) = -D_r \mathcal{R} f(\mathbf{r}, \hat{\mathbf{n}}, t)$ and a contribution from excluded vol-

ume, $\mathcal{J}^X(\mathbf{r}, \hat{\mathbf{n}}, t) = -\frac{D_r}{k_B T} f(\mathbf{r}, \hat{\mathbf{n}}, t) \mathcal{R} V_X(\mathbf{r}, \hat{\mathbf{n}}, t)$, with

$$V_X(\mathbf{r}, \hat{\mathbf{n}}_1, t) = k_B T \int_{s_1} \int_{s_2} \int_{\hat{\mathbf{n}}_2} |\hat{\mathbf{n}}_1 \times \hat{\mathbf{n}}_2| f(\mathbf{r} + \boldsymbol{\xi}, \hat{\mathbf{n}}_2, t), \quad (3)$$

where $\boldsymbol{\xi} = \hat{\mathbf{n}}_1 s_1 - \hat{\mathbf{n}}_2 s_2$ is the separation of the centers of mass of the two filaments and $\int_s \dots = \int_{-\ell/2}^{+\ell/2} ds \dots$ denotes an integration along the length of the filament, parametrized by s . The active contribution to the rotational current (low density approximation) is

$$\mathcal{J}^A(\mathbf{r}, \hat{\mathbf{n}}_1, t) = b^2 \int_{s_1} \int_{s_2} \int_{\hat{\mathbf{n}}_2} \boldsymbol{\omega}^A(\hat{\mathbf{n}}_1, \hat{\mathbf{n}}_2) m(\mathbf{r} + s_1 \hat{\mathbf{n}}_1, t) \times f(\mathbf{r}, \hat{\mathbf{n}}_1, t) f(\mathbf{r} + \boldsymbol{\xi}, \hat{\mathbf{n}}_2, t), \quad (4)$$

where the motor induced angular velocity is written as

$$\boldsymbol{\omega}^A = 2(\gamma_0 + \gamma_1 \hat{\mathbf{n}}_1 \cdot \hat{\mathbf{n}}_2)(\hat{\mathbf{n}}_1 \times \hat{\mathbf{n}}_2). \quad (5)$$

It consists of two parts, corresponding to two classes of motor clusters (see Fig. 1): polar clusters which tend to bind to filaments with similar polarity ($\gamma_0/\gamma_1 \gg 1$)^{4,5}, and non-polar clusters which bind to filament pairs of any orientation ($\gamma_0/\gamma_1 \ll 1$)⁶. Earlier work by two of us¹¹ considered only non-polar clusters ($\gamma_0 = 0$)¹⁷. Both γ_0 and γ_1 will increase with increasing binding rate of the clusters to the filament. A passive polar crosslink (e.g. α -actinin on F-actin) will also have this effect⁸. Since the binding rate can have different dependence on ATP-consumption than the motor stepping speed, we expect a different dependence on ATP hydrolysis rate than the active contributions to the translational currents.

The translational currents are $\mathbf{J}_f = \mathbf{J}^D + \mathbf{J}^X + \mathbf{J}^A$ and

$$\mathbf{J}_m = -D_m \nabla m + \chi \int_s \int_{\hat{\mathbf{n}}} \hat{\mathbf{n}} f(\mathbf{r}, \hat{\mathbf{n}}, t) m(\mathbf{r} + \hat{\mathbf{n}} s, t), \quad (6)$$

where χ depends on the speed and processivity of the motors. The filament diffusive current, $J_i^D = -D_{ij} \partial_j f$, is expressed in terms of a diffusion tensor $D_{ij} = (D_{\parallel} + D_{\perp}) \delta_{ij} / 2 + (D_{\parallel} - D_{\perp}) \hat{Q}_{ij}$ with $\hat{Q}_{ij} = \hat{n}_i \hat{n}_j - \frac{1}{2} \delta_{ij}$. The excluded volume contribution is $J_i^X = -\frac{D_{ij}}{k_B T} f \partial_j V_X$. The active contribution to the translational current is

$$J_i^A(\mathbf{r}, \hat{\mathbf{n}}_1, t) = b^2 \int_{s_1} \int_{s_2} \int_{\hat{\mathbf{n}}_2} v_i^A(\hat{\mathbf{n}}_1, \hat{\mathbf{n}}_2, \boldsymbol{\xi}) m(\mathbf{r} + \hat{\mathbf{n}}_1 s_1, t) \times f(\mathbf{r}, \hat{\mathbf{n}}_1, t) f(\mathbf{r} + \boldsymbol{\xi}, \hat{\mathbf{n}}_2, t), \quad (7)$$

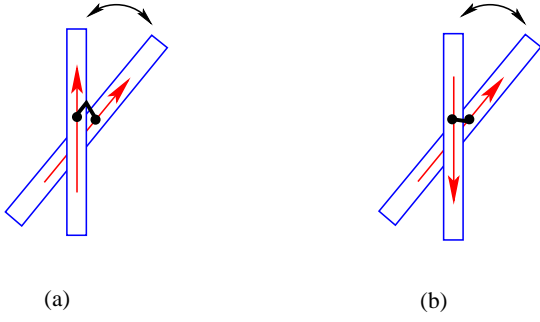


FIG. 1: Polar and nonpolar clusters interacting with polar filaments. Assuming that clusters always bind to the smallest angle, polar clusters ($g \rightarrow \infty$) bind only to filaments in configuration (a) while non-polar clusters ($g = 0$) bind to both configurations equally.

with \mathbf{v}^A the motor-induced velocity, taken of the form

$$\mathbf{v}^A = \frac{\beta}{2}(\hat{\mathbf{n}}_2 - \hat{\mathbf{n}}_1) + \frac{\alpha}{2} \frac{\boldsymbol{\xi}}{2\ell} - \lambda(\hat{\mathbf{n}}_1 + \hat{\mathbf{n}}_2). \quad (8)$$

The parameters α , β and λ have dimensions of velocity and depend on the angle between the filaments. The term proportional to β drives the separation of filaments of opposite polarity, while the λ contribution arises from the net velocity of the filament pair¹⁸. The negative sign reflects the fact that filament mean motion due to motor activity is opposite to their polarity. The contribution proportional to α arises from spatial variations in motor activity along the filament, such as motors stalling before detaching at the polar end. It drives bundling of filaments of the same polarity. These parameters were estimated in Ref.¹⁹ via a microscopic model of motor-induced filament dynamics as $\beta \sim \lambda \sim u_0$, $\alpha \sim u_0(l_m/l) \ll u_0$, with u_0 the mean motor stepping rate and l_m the length scale (of order of the motor cluster size) for spatial variations in motor activity. As seen below, this term is crucial for developing inhomogeneities and pattern formation.

To study the macroscopic properties of the solution, we truncate the exact moment expansion of $f(\mathbf{r}, \hat{\mathbf{n}}, t)$ as

$$f(\mathbf{r}, \hat{\mathbf{n}}, t) = \frac{\rho(\mathbf{r}, t)}{2\pi} \left\{ 1 + 2\mathbf{p}(\mathbf{r}, t) \cdot \hat{\mathbf{n}} + 4S_{ij}(\mathbf{r}, t)\hat{Q}_{ij} \right\}, \quad (9)$$

keeping only the first three moments,

$$\begin{aligned} \int d\hat{\mathbf{n}} f(\mathbf{r}, \hat{\mathbf{n}}, t) &= \rho(\mathbf{r}, t) \quad (\text{density}), \\ \int d\hat{\mathbf{n}} \hat{\mathbf{n}} f(\mathbf{r}, \hat{\mathbf{n}}, t) &= \rho(\mathbf{r}, t)\mathbf{p}(\mathbf{r}, t) \quad (\text{polarization}), \\ \int d\hat{\mathbf{n}} \hat{Q}_{ij} f(\mathbf{r}, \hat{\mathbf{n}}, t) &= \rho(\mathbf{r}, t)S_{ij}(\mathbf{r}, t) \quad (\text{nematic order}). \end{aligned} \quad (10)$$

a. Homogeneous Bulk Steady States. We first consider the dynamical equations for a spatially homogeneous solution. In this case the only contributions to the equation of motion of the filament density come from rotational currents. The motor density has a constant

mean value (we let $m_0 = mb^2$) and the filament density, $f(\mathbf{r}, \hat{\mathbf{n}}, t)$, and its moments can be expressed in terms of their spatial averages, i.e. $\frac{1}{A} \int d\mathbf{r} S_{ij}(\mathbf{r}, t) = S_{ij}(t)$, $\frac{1}{A} \int d\mathbf{r} \mathbf{p}(\mathbf{r}, t) = \mathbf{p}(t)$, with A the area of the system. In the following all lengths are measured in units of the filament length, ℓ . Averaging over the orientation $\hat{\mathbf{n}}$ using Eq. (9), we find that in a homogeneous system $\rho = \rho_0 = \text{constant}$ and

$$\begin{aligned} \partial_t p_i &= -\left(D_r - m_0\rho_0\gamma_0\right)p_i \\ &+ \left[\frac{8D_r}{3\pi} - m_0(2\gamma_0 - \gamma_1)\right]\rho_0 S_{ij}p_j, \end{aligned} \quad (11)$$

$$\begin{aligned} \partial_t S_{ij} &= -\left[4D_r - \frac{8D_r\rho_0}{3\pi} - m_0\rho_0\gamma_1\right]S_{ij} \\ &+ 2m_0\rho_0\gamma_0\left(p_i p_j - \frac{1}{2}\delta_{ij}p^2\right). \end{aligned} \quad (12)$$

In a passive system ($\gamma_0 = \gamma_1 = 0$) there is a transition from an isotropic state to a nematic state. A mean-field description of such a transition, which is continuous in 2d (but first order in 3d), requires that one incorporate cubic terms in the nematic order parameter in the equation of motion. The transition here is identified with the change in sign of the decay rate of S_{ij} , which signals an instability of the isotropic homogeneous state. This occurs when excluded volume effects dominate at a density $\rho_N = 3\pi/2$. The homogeneous state is isotropic for $\rho_0 < \rho_N$ and nematic for $\rho_0 > \rho_N$. No homogeneous polarized state with a nonzero mean value of \mathbf{p} is obtained in a passive solution.

We now turn to an active system. We introduce a dimensionless filament density, $\tilde{\rho} = \rho_0/\rho_N$, a dimensionless motor cluster activity, $\mu = \rho_N m_0 \gamma_1 / D_r$, and a parameter measuring the polarity of motor clusters, $g = \gamma_0/\gamma_1$ with $g = 0$ corresponding to non-polar clusters. Time is measured in units of D_r^{-1} . The steady states of Eqs. (11) and (12) are the stable solutions of

$$0 = -a_1 p_i + b_1 \tilde{\rho} S_{ij} p_j, \quad (13)$$

$$0 = -a_2 S_{ij} + b_2 \tilde{\rho} \left(p_i p_j - \frac{1}{2}\delta_{ij} p^2\right), \quad (14)$$

where

$$a_1 = 1 - \tilde{\rho} g \mu, \quad (15)$$

$$a_2 = 4[1 - \tilde{\rho}(1 + \mu/4)], \quad (16)$$

and $b_1 = 4 + \mu(1 - 2g)$, $b_2 = 2g\mu$. At low density the only solution is $p_i = 0$ and $S_{ij} = 0$ and the system is isotropic (I). The homogeneous isotropic state can become unstable in two ways. As in the passive case, a change in sign of the coefficient a_2 signals the transition to a nematic (N) state. Motor activity lowers the density for the I-N transition which occurs at $\rho_{IN}(\mu) = 1/(1 + \mu/4)$. At $\tilde{\rho} > \rho_{IN}(\mu)$ the solution acquires nematic order, with $S_{ij}^0 = S_0(n_i n_j - \delta_{ij}/2)$, where the unit vector \mathbf{n} denotes the direction of broken symmetry. We obtain an expression for the amount of nematic order (S_0) by

adding a cubic term $-c_2\tilde{\rho}^2S_{kl}S_{kl}S_{ij}$ to Eq. (14) giving $S_0 = \frac{1}{\tilde{\rho}}\sqrt{-2a_2/c_2}$. The isotropic state can also become linearly unstable via the growth of polarization fluctuations in any arbitrary direction. This occurs above a second critical filament density, $\rho_{IP}(\mu) = 1/(g\mu)$, defined by the change in sign of the coefficient a_1 controlling the decay of polarization fluctuations. For $\tilde{\rho} > \rho_{IP}(\mu)$ the homogeneous state is polarized (P), with $p_i \neq 0$. The alignment tensor also have a nonzero mean value in the polarized state as it is slaved to the polarization. One can identify two scenarios depending on the value of g .

I) For $g < 1/4$, the density ρ_{IP} is always larger than ρ_{IN} and a region of nematic phase exists for all values of μ . At sufficiently high filament and motor densities, the nematic state also becomes unstable. Fluctuations in the alignment tensor are uniformly stable for $a_2 < 0$, but polarization fluctuations along the direction of broken symmetry become unstable for $a_1 \leq \tilde{\rho}b_1S_0/2$, i.e., above a critical density

$$\rho_{NP} = \frac{1}{g\mu} \left[1 + \frac{b_1^2}{c_2R} \left(1 - \sqrt{1 + \frac{2c_2R(1-R)}{b_1^2}} \right) \right] \quad (17)$$

where $R = \rho_{IN}/\rho_{IP}$. The polarized state at $\tilde{\rho} > \rho_{NP}$ has $p_i^0 = p_0n_i$ and $S_{ij}^0 = S_P(n_in_j - \delta_{ij}/2)$, where $p_0^2 = \frac{2a_1a_2}{\tilde{\rho}^2b_1b_2} \left[1 - \left(\frac{2a_1}{b_1S_0} \right)^2 \right]$ and $S_P = S_0\sqrt{1 - \frac{\tilde{\rho}^2b_1b_2}{2a_1a_2}p_0^2} = 2|a_1/b_1|$. The "phase diagram" is shown in Fig. 2.

II) When $g > 1/4$, the boundaries for the I-N and the N-P transitions cross at $\mu_x = 1/(g - 1/4)$ where $\rho_{IN} = \rho_{IP} = \rho_{NP}$ and the phase diagram has the topology shown in Fig. 3. For $\mu > \mu_x$ the system goes directly from the I to the P state at ρ_{IP} , without an intervening N state. At the onset of the polarized state the alignment tensor is again slaved to the polarization field, $\rho_0S_{ij} = \frac{b_2}{a_2} (p_ip_j - \frac{1}{2}\delta_{ij}p^2)$, and $p_i = p_0n_i$ and p_0 is determined by cubic terms in Eq. 11.

If $\gamma_1 = 0$, with $\gamma_0 \neq 0$, the I-N transition is independent of motor density and always occurs at $\rho_0 = \rho_N$.

b. Spatially inhomogeneous states. Spatial inhomogeneities of course affect the stability of the homogeneous states described above. As shown by several authors, the rate of motor-induced filament bundling can exceed that of filament diffusion yielding the unstable growth of density inhomogeneities^{7,9,10,11}. States with spatially varying orientational order, where the filaments spontaneously arrange in vortex and aster structures, are also possible^{12,15,16}. To examine the role of spatial inhomogeneities, we have obtained coupled equations for the first three moments of the filament concentration defined in Eq. (9) by an expansion in spatial gradients described elsewhere^{11,19}. These equations can then be used to study the linear stability of each of the homogeneous states against the growth of spatially-varying fluctuations in the hydrodynamic fields. These are the fields whose characteristic decay time are much longer than any microscopic relaxation time and become infinitely long lived at long wavelengths. We find that the low frequency hydrodynamic modes of this active system are determined by fluctuations in the conserved densities and in variables associated with broken symmetries. A change in sign in the decay rate of these modes signals an instability of the macroscopic state of interest. For simplicity we only discuss here the case of constant motor density.

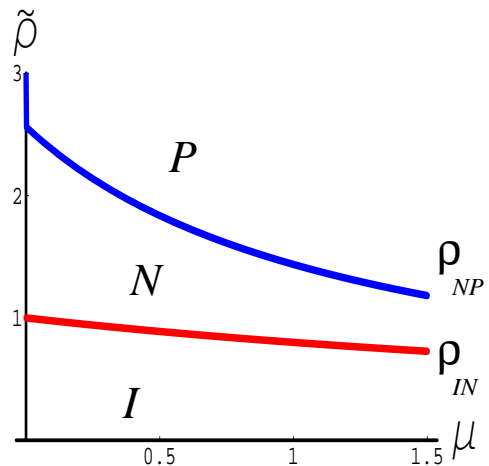


FIG. 2: The homogeneous phase diagram for $g < 1/4$ (the figure is for $g = 1/10$ and $c_2 = 50$). The vertical axis is ρ_0/ρ_N , the horizontal axis is μ .

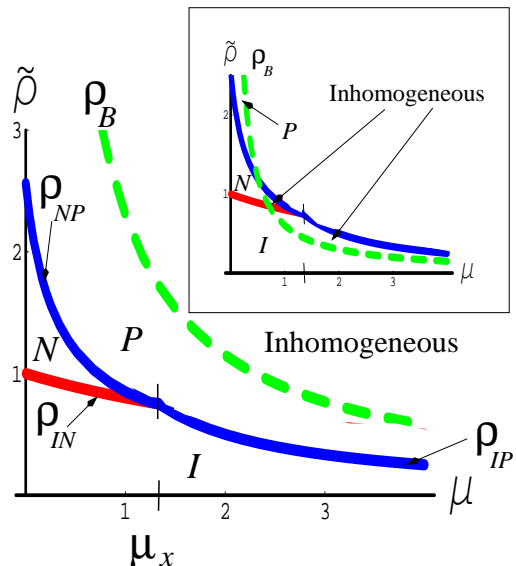


FIG. 3: The phase diagram for $g > 1/4$. For $\mu > \mu_x$, where ρ_{IN} and ρ_{IP} intersect, no N state exists and the system goes directly from the I to the P state. Inhomogeneous states form for $\rho_0 > \rho_B$. The ρ_B line may lie above the $\rho_{NP} - \rho_{IP}$ line, as shown in the main figure ($g = 1$, $\gamma_1/\alpha = 2.3$), or cross through the N and I states, as shown in the inset ($g = 1$, $\gamma_1/\alpha = 0.6$), depending on the value of γ_1/α . (with $c_2 = 50$).

hydrodynamic modes of this active system are determined by fluctuations in the conserved densities and in variables associated with broken symmetries. A change in sign in the decay rate of these modes signals an instability of the macroscopic state of interest. For simplicity we only discuss here the case of constant motor density.

Isotropic state. This has been studied in Ref¹¹. The only hydrodynamic variable is the filament density, ρ . The decay rate of Fourier components of $\delta\rho = \rho - \rho_0$ at wavevector k is controlled by the interplay of diffu-

sion and motor-induced filament bundling described by α . The homogeneous I state is unstable at large length scales for $\rho_0 > \rho_B$, with $\rho_B \sim D_{\parallel}/(m_0\alpha) \sim \gamma_1/(\alpha\mu)$. The homogeneous state is stabilized at short scales by excluded volume corrections and higher order terms in the density gradients. The density instability is driven entirely by the bundling rate α , while β plays no role.

Polarized state. The hydrodynamic modes in the P state are those associated with fluctuations in the filament density and in the director field, $\mathbf{n}(\mathbf{r}, t)$, defined by $\mathbf{p}(\mathbf{r}, t) = p(\mathbf{r}, t)\mathbf{n}(\mathbf{r}, t)$, with $|\mathbf{n}| = 1$. The coupled hydrodynamic modes describing the decay of Fourier components of density, $\delta\rho$ and director fluctuations, $\delta\mathbf{n} = \mathbf{n} - \hat{\mathbf{y}} = \hat{\mathbf{x}}\delta n_x$ of wavevector \mathbf{k} are always propagating, with velocity whose magnitude and direction are controlled by *both* the activity parameters β and λ . For \mathbf{k} along the broken symmetry direction, the modes decouple (i.e., $\delta\rho \sim e^{z_\rho(k)t}$, $\delta n_x \sim e^{z_n(k)t}$) and are given by

$$z_\rho = ikc_1\tilde{\rho}\mu\tilde{\beta} - \frac{k^2}{8}\left[1 - \frac{g\mu}{6} - 20\tilde{\rho}\mu\tilde{\alpha}\right], \quad (18)$$

$$z_n = -ikc_2\tilde{\rho}\mu\tilde{\beta} - \frac{5k^2}{48}\left[1 + \frac{2}{5}\tilde{\rho}\mu(g - 6\tilde{\alpha})\right], \quad (19)$$

where $\tilde{\beta} = \beta/\gamma_1$, $\tilde{\alpha} = \alpha/\gamma_1$, and c_1 and c_2 are numbers of order one. We have used $D_{\parallel} = \ell^2 D_r/6$ and $\lambda \sim \beta$. Like the I state, the homogeneous P state is linearly unstable for $\rho_0 > \rho_B$. The nature of the instability changes, however, from diffusive in the I state to oscillatory in the P state, suggesting that spatially inhomogeneous oscillatory structures, such as vortices, may be stable at high filament or motor densities. The rotational effects described by $\mu \sim \gamma_1$ stabilize director fluctuations, but destabilize the density.

Nematic state. The hydrodynamic variables in the N state are again the filament density and a director field $\mathbf{n}(\mathbf{r}, t)$, defined in terms of the alignment tensor as $S_{ij} = S_0(n_i n_j - \frac{1}{2}\delta_{ij})$. The decay of density and director fluctuations is controlled by coupled hydrodynamic

modes which are always diffusive. The modes decouple for \mathbf{k} along the broken symmetry direction, with

$$z_\rho = -k^2\left[\frac{1}{6} - 2\tilde{\rho}\mu\tilde{\alpha}\right], \quad (20)$$

$$z_n = -\frac{k^2}{8}\left[1 + \frac{19}{36}\tilde{\rho}\mu\right]. \quad (21)$$

Once again, the homogeneous N state is destabilized by the growth of density fluctuations for $\rho_0 > \rho_B$, while long wavelength director fluctuations remain stable. For arbitrary direction of \mathbf{k} relative to the direction of broken symmetry director fluctuations also become unstable at high density, but the fastest growing mode is always associated with the build-up of density inhomogeneities. In contrast to the P state, the instability is always diffusive.

To summarize, we have studied the phase behavior of polar filaments interacting with polar clusters. We have shown that in addition to the homogeneous *isotropic* phase, both homogeneous *polarized* and *nematic* states can be obtained as a function of filament density and motor activity and polarity. The instabilities of the homogeneous states are controlled by the bundling rate α and occur for $\rho_0 > \rho_B \sim \gamma_1/(\alpha\mu)$. The location of this line in the phase diagram depends crucially on the parameter γ_1/α . If $\gamma_1/\alpha > 1/g = \gamma_1/\gamma_0$, then $\rho_B > \rho_P$ as shown in Fig. 3, and the homogeneous nematic state is always stable, when it exists. If $\gamma_1/\alpha < 1/g = \gamma_1/\gamma_0$, then $\rho_B < \rho_P$ as shown in the inset of Fig. 3, and all homogeneous states can be destabilized by filament bundling, albeit through different (diffusive versus oscillatory) mechanisms.

Acknowledgments

TBL acknowledges the support of the Royal Society. MCM acknowledges support from the National Science Foundation, grants DMR-0305407 and DMR-0219292.

¹ B. Alberts et al., *Molecular Biology of the Cell* (Garland, New York, 2002).
² J. Howard, *Mechanics of Motor Proteins and the Cytoskeleton* (Sinauer, New York, 2000).
³ K. Takiguchi, *J. Biochem.* **109**, 520 (1991); R. Urrutia et al., *PNAS* **88**, 6701 (1991).
⁴ F. J. Nédélec et al, *Nature* **389**, 305 (1997).
⁵ T. Surrey et al, *Science* **292**, 1167 (2001).
⁶ D. Humphrey et al, *Nature* (London) **416**, 412 (2002).
⁷ H. Nakazawa and K. Sekimoto, *J. Phys. Soc. Jpn.* **65**, 2404 (1996).
⁸ M. Tempel, G. Isenberg and E. Sackmann, *Phys. Rev. E.* **54**, 1802-1810 (1996).
⁹ K. Kruse and F. Jülicher, *Phys. Rev. Lett.* **85**, 1778 (2000); *Phys. Rev. E.* **67**, 051913 (2003).
¹⁰ K. Kruse, S. Caialet, and F. Jülicher, *Phys. Rev. Lett.* **87**, 138101 (2001).
¹¹ T. B. Liverpool and M. C. Marchetti, *Phys. Rev. Lett.* **90**,

138102 (2003); *ibid* **93**, 159802 (2004). F. Ziebert and W. Zimmerman, *Phys. Rev. Lett.* **93**, 159801 (2004).
¹² H. Y. Lee and M. Kardar, *Phys. Rev. E* **64**, 56113 (2001).
¹³ R. A. Simha and S. Ramaswamy, *Phys. Rev. Lett.* **89**, 058101 (2002).
¹⁴ K. Kruse et al., *Phys. Rev. Lett.* **92**, 078101 (2004).
¹⁵ S. Sankararaman et al, *Phys. Rev. E* **70**, 031905 (2004)
¹⁶ I. S. Aranson and L. S. Tsimring, *Phys. Rev. E* **71**, 50901(R) (2005).
¹⁷ A simple model of the cluster as a torsional spring of constant κ gives a typical scale for $\gamma_0 \sim D_r\kappa/k_B T$.
¹⁸ It was shown in Ref.¹⁹ that due to the anisotropy of the diffusion tensor of rods the motor cluster can induce a net velocity of the filament pair even without external forces.
¹⁹ T.B. Liverpool and M. C. Marchetti, *Europhys. Lett.* **69**, 846 (2005).